

Communication

# Second-Order Statistics of Partially Coherent Beams with Laguerre Non-Uniform Coherence Properties under Turbulence

Yang Zhao <sup>1</sup>, Zhiwen Yan <sup>1,2,3</sup>, Yibo Wang <sup>1</sup>, Liming Liu <sup>1,2,3</sup>, Xinlei Zhu <sup>1,2,3</sup>, Bohan Guo <sup>1,2,3,\*</sup> and Jiayi Yu <sup>1,2,3,\*</sup> 

<sup>1</sup> Shandong Provincial Engineering and Technical Center of Light Manipulation & Shandong Provincial Key Laboratory of Optics and Photonic Devices, School of Physics and Electronics, Shandong Normal University, Jinan 250358, China

<sup>2</sup> Collaborative Innovation Center of Light Manipulation and Applications, Shandong Normal University, Jinan 250358, China

<sup>3</sup> Joint Research Center of Light Manipulation Science and Photonic Integrated Chip of East China Normal University and Shandong Normal University, East China Normal University, Shanghai 200241, China

\* Correspondence: bohanguo@sdu.edu.cn (B.G.); jiayiyu0528@sdu.edu.cn (J.Y.)

**Abstract:** We use the extended Huygens–Fresnel integral to analyze the propagation properties of a class of partially coherent beams with Laguerre non-uniform coherence properties (called Laguerre non-uniformly correlated beams) in free space and in a turbulent atmosphere. We focus on how different initial beam orders and coherence lengths affect the propagation behavior of the beams, such as the evolution of intensity, degree of coherence, propagation factor, and beam wander. Our results show that non-uniform coherence properties play a role in resisting the degrading effects of turbulence. Furthermore, adjusting the initial beam parameter of the non-uniform coherence structure, i.e., increasing the beam order and decreasing the coherence, can further improve the turbulence resistance of the beams. Our results have potential applications in free-space optical communications.

**Keywords:** non-uniformly correlated beam; propagation; turbulence



**Citation:** Zhao, Y.; Yan, Z.; Wang, Y.; Liu, L.; Zhu, X.; Guo, B.; Yu, J. Second-Order Statistics of Partially Coherent Beams with Laguerre Non-Uniform Coherence Properties under Turbulence. *Photonics* **2023**, *10*, 837. <https://doi.org/10.3390/photronics10070837>

Received: 30 June 2023

Revised: 18 July 2023

Accepted: 19 July 2023

Published: 20 July 2023



**Copyright:** © 2023 by the authors. Licensee MDPI, Basel, Switzerland. This article is an open access article distributed under the terms and conditions of the Creative Commons Attribution (CC BY) license (<https://creativecommons.org/licenses/by/4.0/>).

## 1. Introduction

Light beams modulated by spatial characteristics have been described as spatially structured beams, which exhibit some innovative optical features due to some special spatial structures [1]. In addition to amplitude, polarization, and phase, spatial coherence is another important spatial fundamental nature of light beams, which describes the degree of correlation of fields at two different positions in a spatial field and plays an important role in understanding the interaction between light and matter [2–4]. Partially coherent beams (PCBs) with reduced spatial coherence can not only maintain the propagation characteristics of their original coherent beams but also have weaker diffraction or interference effects due to their low coherence; furthermore, the coherence structure of PCBs can induce some novel physics features [5–9], which means that PCBs have important potential applications in many fields [3–5]. As a branch of microwave communication, free-space optical (FSO) communication is usually referred to as the use of laser as the carrier of communication technology [10]. Choosing the coherence structure of PCBs as an effective strategy for encoding and transmitting information has important application potential in FSO communication [11,12]. However, when the laser beams pass through a turbulent atmosphere, the beam dynamics are largely impacted by the turbulence, leading to a series of negative effects such as beam expansion, beam wander, and scintillation, thereby reducing the effectiveness of FSO communication systems [13–15]. Therefore, the propagation features of PCBs in a turbulent atmosphere and the research on decreasing the adverse impact of turbulence have become a research hotspot.

A large class of PCBs has spatially variable coherence structure functions, labeled as non-uniformly correlated beams [16–20]. This coherence feature differentiates these beams

from conventional uniformly correlated beams in terms of their propagation traits. The research on non-uniformly correlated beams can be traced back to the beginning of the 21st century. However, since then, few papers have been on non-uniformly correlated beams due to mathematical difficulties. In 2007, F. Gori et al. introduced the necessary and sufficient conditions for constructing partially coherent sources [21]. Afterward, Lajunen et al. constructed conventional non-uniformly correlated beams [17]. These beams have the propagation characteristics of lateral shift of intensity and self-focusing on propagation. Subsequently, Y. Gu and G. Gbur investigated the propagation features of such beams in a turbulent atmosphere, which have lower intensity scintillation and higher intensity on-axis. These results are significant because uniformly correlated PCBs often have disadvantages such as large divergence angles and serious energy dissipation when propagating in turbulence [22]. In 2018, J. Yu et al. constructed more general non-uniformly correlated beams, added configurable non-uniform correlation structure parameters, and studied the intensity and correlation structure of Hermitian non-uniformly correlated beams under a turbulent atmosphere [18,19]. In 2020, J. Yu et al. introduced non-uniform polarization structures into non-uniformly correlated beams, exhibiting self-healing properties of the intensity and polarization in a turbulent atmosphere [20,23]. Although the above results obtained some new propagation properties, only a few studies exist on beam quality indicators, such as propagation factor and beam wander, which are considered global parameters for determining beam quality.

In this report, we selected a class of non-uniform correlated beams with Laguerre non-uniform correlation structure as the research object and studied their evolution of the intensity and degree of coherence (DOC) in free space and turbulence. Moreover, the second-order moments of such beams in turbulence are estimated, as well as the propagation factor and beam wander of the proposed beams. The findings will facilitate the application of non-uniform correlation structure manipulation in FSO communications. In Section 2, the analytical expressions of cross-spectral density (CSD), propagation factor and beam wander of Laguerre non-uniformly correlated (LNUC) beams in turbulence are derived based on the extended Huygens–Fresnel principle and the Wigner distribution function. In Section 3, the numerical calculation and results are presented and discussed. In Section 4, the conclusion and discussion are presented.

## 2. Analytical Formulas of the Laguerre Non-Uniformly Correlated Beams in Turbulence

The paraxial propagation of a PCB under turbulence can be described by the extended Huygens–Fresnel integral [10]:

$$W(\boldsymbol{\rho}_1, \boldsymbol{\rho}_2) = \frac{1}{\lambda^2 z^2} \iint W_0(\mathbf{r}_1, \mathbf{r}_2) \exp\left[-\frac{ik}{2z}(\mathbf{r}_1 - \boldsymbol{\rho}_1)^2 + \frac{ik}{2z}(\mathbf{r}_2 - \boldsymbol{\rho}_2)^2\right] \times \langle \exp[\Psi^*(\mathbf{r}_1, \boldsymbol{\rho}_1) + \Psi(\mathbf{r}_2, \boldsymbol{\rho}_2)] \rangle d^2\mathbf{r}_1 d^2\mathbf{r}_2, \tag{1}$$

where  $\mathbf{r} \equiv (x, y)$  and  $\boldsymbol{\rho} \equiv (\rho_x, \rho_y)$  are the transverse position vector in the source and target plane, respectively.  $W_0(\mathbf{r}_1, \mathbf{r}_2)$  and  $W(\boldsymbol{\rho}_1, \boldsymbol{\rho}_2)$  are the CSD of the selected beam in the source and target plane, respectively.  $k = 2\pi/\lambda$  is the wavenumber, where  $\lambda$  denotes the wavelength.  $\Psi(\mathbf{r}, \boldsymbol{\rho})$  is the complex phase disturbance induced by the turbulent medium. The ensemble average over the turbulence of the last term can be expressed as [10]

$$\langle \exp[\Psi^*(\mathbf{r}_1, \boldsymbol{\rho}_1) + \Psi(\mathbf{r}_2, \boldsymbol{\rho}_2)] \rangle = \exp\left\{-\left(\frac{\pi^2 k^2 z T}{3}\right) \left[ (\boldsymbol{\rho}_1 - \boldsymbol{\rho}_2)^2 + (\boldsymbol{\rho}_1 - \boldsymbol{\rho}_2) \cdot (\mathbf{r}_1 - \mathbf{r}_2) + (\mathbf{r}_1 - \mathbf{r}_2)^2 \right] \right\}, \tag{2}$$

with  $T = \int_0^\infty \kappa^3 \Phi_n(\kappa) d^2\kappa$ , in which  $\Phi_n(\kappa)$  represents the spatial power spectrum of the turbulence.

Now, we focused on a particular example of spatially structured sources whose correlation function is an inhomogeneous function of Laguerre form; here, we named it

LNUC sources. Such sources can be expressed in terms of the Cartesian coordinate system, which is as follows [24]:

$$W_0(\mathbf{r}_1, \mathbf{r}_2) = \exp\left(-\frac{\mathbf{r}_1^2 + \mathbf{r}_2^2}{2w_0^2}\right) \mu(\mathbf{r}_1, \mathbf{r}_2), \tag{3}$$

where  $w_0$  refers to the beam width. The correlation function  $\mu(\mathbf{r}_1, \mathbf{r}_2)$  is given by [24]

$$\mu(\mathbf{r}_1, \mathbf{r}_2) = L_n^0 \left[ \frac{(\mathbf{r}_1^2 - \mathbf{r}_2^2)^2}{\delta^4} \right] \exp\left[-\frac{(\mathbf{r}_1^2 - \mathbf{r}_2^2)^2}{\delta^4}\right]. \tag{4}$$

where  $L_n^0$  represents the Laguerre polynomial of modes  $n$  and 0,  $\delta$  refers to the coherence length.

While Equations (3) and (4) are substituted into Equation (1) for direct integral operation, the operation process is extremely complicated, and high-order terms will appear in the process, making it difficult to obtain the final analytical solution. In order to avoid complex calculations, we reset the beam model to achieve the purpose of reducing the power. According to the construction of partially coherent sources, their CSD can be represented via the integral as [21]

$$W(\mathbf{r}_1, \mathbf{r}_2) = \int p(\mathbf{v}) h^*(\mathbf{r}_1, \mathbf{v}) h(\mathbf{r}_2, \mathbf{v}) d^2\mathbf{v}, \tag{5}$$

where  $p(\mathbf{v})$  is a non-negative function for any one-dimensional variable  $\mathbf{v}$ , and  $h(\mathbf{r}, \mathbf{v})$  can be taken as any kernel function. In practical cases,  $h(\mathbf{r}, \mathbf{v})$  is the response function of an optical system, which can be expressed as follows [24]:

$$h(\mathbf{r}, \mathbf{v}) = \exp\left(-\frac{\mathbf{r}^2}{2w_0^2}\right) \exp\left[-ik(v_x + v_y)\mathbf{r}^2\right], \tag{6}$$

$$p(\mathbf{v}) = \left(\frac{\alpha^{n+1}}{\pi n!}\right) \mathbf{v}^{2n} \exp(-\alpha\mathbf{v}^2), \tag{7}$$

with  $\alpha = k^2\delta^4/2$ .

Considering the necessary and sufficient condition shown in Equation (5) as discretization, the PCBs can be regarded as an incoherent superposition of coherent modes. Therefore, the propagation behavior of each coherent mode in turbulence can be considered first, and then they are superposed incoherently. Substituting Equation (5) into Equation (1), we have the following form:

$$W(\boldsymbol{\rho}_1, \boldsymbol{\rho}_2) = \int p(\mathbf{v}) H(\boldsymbol{\rho}_1, \boldsymbol{\rho}_2, \mathbf{v}) d^2\mathbf{v}, \tag{8}$$

where  $H(\boldsymbol{\rho}_1, \boldsymbol{\rho}_2, \mathbf{v})$  denotes the results of the coherent modes after propagation,

$$H(\boldsymbol{\rho}_1, \boldsymbol{\rho}_2, \mathbf{v}) = w_0^2 w_z^{-2} \exp\left[-i\chi w_0^{-1}(\boldsymbol{\rho}_1^2 - \boldsymbol{\rho}_2^2)/2\right] \exp\left[-(\chi^2/4 + \Omega)(\boldsymbol{\rho}_1 - \boldsymbol{\rho}_2)^2\right] \times \exp\left[w_0 w_z^{-1} \chi [1 - (v_x + v_y)z - 2\Omega](\boldsymbol{\rho}_1 - \boldsymbol{\rho}_2) + i w_z^{-1}(\boldsymbol{\rho}_1 + \boldsymbol{\rho}_2)\right], \tag{9}$$

where

$$\chi = w_0 k z^{-1}; \quad \Omega = \pi^2 k z^2 T/3; \quad w_z^2 = w_0^2 [1 - 2(v_x + v_y)z]^2 + \chi^{-2} + 4w_0 \chi^{-1} \Omega. \tag{10}$$

We now have the intensity and DOC of LNUC beams

$$S(\boldsymbol{\rho}) = W(\boldsymbol{\rho}, \boldsymbol{\rho}) = \int \frac{w_0^2}{w_z^2} p(\mathbf{v}) \exp\left(-\frac{\boldsymbol{\rho}^2}{w_z^2}\right) d^2\mathbf{v}, \tag{11}$$

and

$$\mu(\rho_1, \rho_2) = \frac{W(\rho_1, \rho_2)}{\sqrt{S(\rho_1)S(\rho_2)}}. \tag{12}$$

To further study the propagation features of PCBs, we have two global parameters: propagation factor and beam wander. Both of them are related to the second-order moments of the beams. The second-order moments of PCBs in turbulence can be obtained from the following expressions [25]:

$$\langle \rho^2 \rangle = \langle r^2 \rangle_0 + 2\langle \mathbf{r} \cdot \boldsymbol{\theta} \rangle_0 z + \langle \theta^2 \rangle_0 z^2 + \frac{4\pi^2 T z^3}{3}, \tag{13}$$

$$\langle \theta^2 \rangle = \langle \theta^2 \rangle_0 + 4\pi^2 T z, \tag{14}$$

$$\langle \boldsymbol{\rho} \cdot \boldsymbol{\theta} \rangle = \langle \mathbf{r} \cdot \boldsymbol{\theta} \rangle_0 + \langle \theta^2 \rangle_0 z + 2\pi^2 T z^2, \tag{15}$$

where  $\boldsymbol{\theta} = (\theta_x, \theta_y)$ ,  $r = |\mathbf{r}|$ ,  $\rho = |\boldsymbol{\rho}|$  and  $\theta = |\boldsymbol{\theta}|$ . The quantities  $\langle r^2 \rangle_0$ ,  $\langle \mathbf{r} \cdot \boldsymbol{\theta} \rangle_0$  and  $\langle \theta^2 \rangle_0$  denote the second-order moments of a PCB in the source plane, and the integrals can obtain them [26]

$$\langle r^2 \rangle_0 = \frac{1}{I} \int_0^{2\pi} \int_0^\infty r^3 W_0(r, \theta, r, \theta) dr d\theta, \tag{16}$$

$$\langle \theta^2 \rangle_0 = \frac{1}{k^2 I} \int_0^{2\pi} \int_0^\infty \left\{ \frac{\partial^2 W_0(r_1, \theta_1, r_2, \theta_2)}{\partial r_1 \partial r_2} \Big|_{\theta_1=\theta_2=\theta}^{r_1=r_2=r} + \frac{1}{r^2} \frac{\partial^2 W_0(r_1, \theta_1, r_2, \theta_2)}{\partial \theta_1 \partial \theta_2} \Big|_{\theta_1=\theta_2=\theta}^{r_1=r_2=r} \right\} r dr d\theta, \tag{17}$$

$$\langle \mathbf{r} \cdot \boldsymbol{\theta} \rangle_0 = \frac{1}{ikI} \int_0^{2\pi} \int_0^\infty \left\{ r_1 \frac{\partial W_0(r_1, \theta_1, r_2, \theta_2)}{\partial r_1} - r_2 \frac{\partial W_0(r_1, \theta_1, r_2, \theta_2)}{\partial r_2} \right\} \Big|_{\theta_1=\theta_2=\theta}^{r_1=r_2=r} r dr d\theta, \tag{18}$$

where  $I$  is the average energy for the beam in the target plane

$$I = \int_0^{2\pi} \int_0^\infty W(r, \theta, r, \theta) r dr d\theta. \tag{19}$$

Therefore, by substituting the CSD of LNUC source, i.e., Equation (3), into the above formulas, the second-order moments of LNUC beams in turbulence can be obtained

$$\langle \rho^2 \rangle = w_0^2/2 + 2\chi^{-2} + 4w_0^4\chi^{-2}\delta^{-4} \left( L_{n-1}^1(0) + 1 \right) + 4\pi^2 T z^3/3, \tag{20}$$

$$\langle \theta^2 \rangle = 2\chi^{-2}z^{-2} + 4w_0^2k^{-2}\delta^{-4} \left( L_{n-1}^1(0) + 1 \right) + 4\pi^2 T z, \tag{21}$$

$$\langle \boldsymbol{\rho} \cdot \boldsymbol{\theta} \rangle = 2\chi^{-2}z^{-1} + 4w_0^2k^{-2}\delta^{-4}z \left( L_{n-1}^1(0) + 1 \right) + 2\pi^2 T z^2. \tag{22}$$

Gori et al. defined the propagation factor as the following form, which is related to the second-order moments [27]:

$$M^2(z) = \sqrt{\langle \rho^2 \rangle \langle \theta^2 \rangle - \langle \boldsymbol{\rho} \cdot \boldsymbol{\theta} \rangle^2}. \tag{23}$$

Beam wander describes the variance of the instantaneous center displacement in turbulence, is defined by Andrews and Phillips as [28]

$$\langle r_c^2 \rangle = 4\pi k^2 W_{FS}^2 \int_0^L \int_0^\infty \kappa \Phi_n(\kappa) \exp\left(-\kappa^2 W_{LT}^2\right) \left\{ 1 - \exp\left[-\frac{2L^2\kappa^2(1-z/L)^2}{k^2 W_{FS}^2}\right] \right\} d\kappa dz. \tag{24}$$

Here, we model the turbulence using the von Karman power spectrum [29]

$$\Phi_n(\kappa) = A(\alpha)C_n^2(\kappa^2 + \kappa_0^2)^{-\alpha/2} \exp(-\kappa^2/\kappa_m^2), \tag{25}$$

where  $A(\alpha) = \Gamma(\alpha - 1)\cos(\alpha\pi/2)/(4\pi^2)$  with  $\Gamma$  denotes the Gamma function,  $\kappa_0 = 2\pi/L_0$  and  $\kappa_m = [2\pi A(\alpha)\Gamma(5 - \alpha/2)]^{1/(\alpha-5)}/l_0$  with  $L_0$  and  $l_0$  being the outer and inner scale of turbulence.

Substituting Equation (25) into Equation (24), the expression for the beam wander in turbulence is obtained by geometrical optics approximation

$$\langle r_c^2 \rangle = \frac{4\pi^2 C_n^2 A(\alpha) L^2}{(\alpha-2)} \kappa_0^{-\alpha} \int_0^L (1 - \frac{z}{L})^2 \left\{ -2\kappa_0^4 + \kappa_0^\alpha \kappa_m^2 (W_{LT}^2 + \kappa_m^{-2})^{\alpha/2} (1 + \kappa_m^2 W_{LT}^2)^{-2} \right. \\ \left. [2\kappa_0^2 (1 + \kappa_m^2 W_{LT}^2) + (\alpha - 2)\kappa_m^2] \exp\left[ \left(\frac{\kappa_0}{\kappa_m}\right)^2 + \kappa_0^2 W_{LT}^2 \right] \Gamma\left[ 2 - \frac{\alpha}{2}, \left(\frac{\kappa_0}{\kappa_m}\right)^2 + \kappa_0^2 W_{LT}^2 \right] \right\} dz. \tag{26}$$

Notably, the source parameters determine the beam wander.  $W_{LT}$ , the mean-square beam width of the beams in turbulence, can only be controlled, i.e.,  $W_{LT}^2 = \langle \rho^2 \rangle$ .

### 3. Statistical Properties of LNUC Beams

The statistical properties of LUNC beams can be calculated using the above-mentioned analysis. Unless otherwise stated, we set the initial beam and turbulence parameters as follows:  $\lambda = 632.8$  nm,  $w_0 = 5$  cm,  $L_0 = 1$  m,  $l_0 = 1$  mm,  $\alpha = 11/3$ , and  $C_n^2 = 10^{-15} \text{ m}^{-2/3}$ . For convenience, the wavelength was taken to be that of common HeNe-type laser diodes; the results presented here are qualitatively similar for optical communications wavelengths.

#### 3.1. In the Source Plane

Figure 1a,b depict the absolute value distribution of the DOC of LNUC sources in the  $x_1$ - $x_2$  plane with  $y_1 = y_2 = 0$  and in the  $x_1$ - $y_1$  plane with  $x_2 = y_2 = 0$ , respectively. We found that such sources exhibit high coherence with an “X” distribution in the  $x_1$ - $x_2$  plane and show circular symmetry and highly coherence regions in the  $x_1$ - $y_1$  plane. Comparing the subgraphs in Figure 1a,b, we found that the number of side lobes increases with the increase in beam order values.

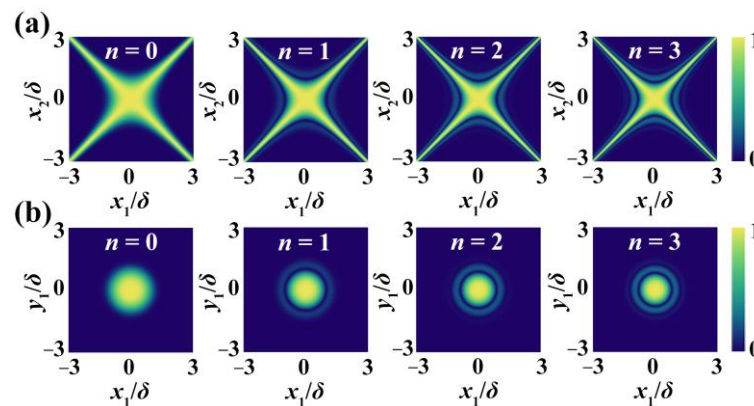


**Figure 1.** Distribution of the DOC of LNUC sources (a) in the  $x_1$ - $x_2$  plane with  $y_1 = y_2 = 0$ ; (b) in the  $x_1$ - $y_1$  plane with  $x_2 = y_2 = 0$ .

#### 3.2. Propagation in Free Space

Figure 2 depicts the evolution of the normalized intensity of the LNUC beams propagating in free space. The intensity is normalized by setting the on-axis intensity of the source to unity. Figure 2a shows a prominent intensity peak in propagation, which indicates that the LNUC beam exhibits self-focusing properties. According to Figure 2b,c, the on-axis intensity depends on the initial beam order and coherence length, respectively. Based on the numerical results, the on-axis intensity increases to a maximum and then gradually

decreases, indicating that the beam exhibits self-focusing features during propagation. This conclusion matches with the results obtained from Figure 2a. Furthermore, we ensured that the intensity peak of the beam increases with increasing beam order and decreasing coherence and that the intensity peak of the beam increases with increasing beam order and decreasing coherence, which is similar to the behavior of Hermite non-uniformly correlated beams discussed in [20,21].

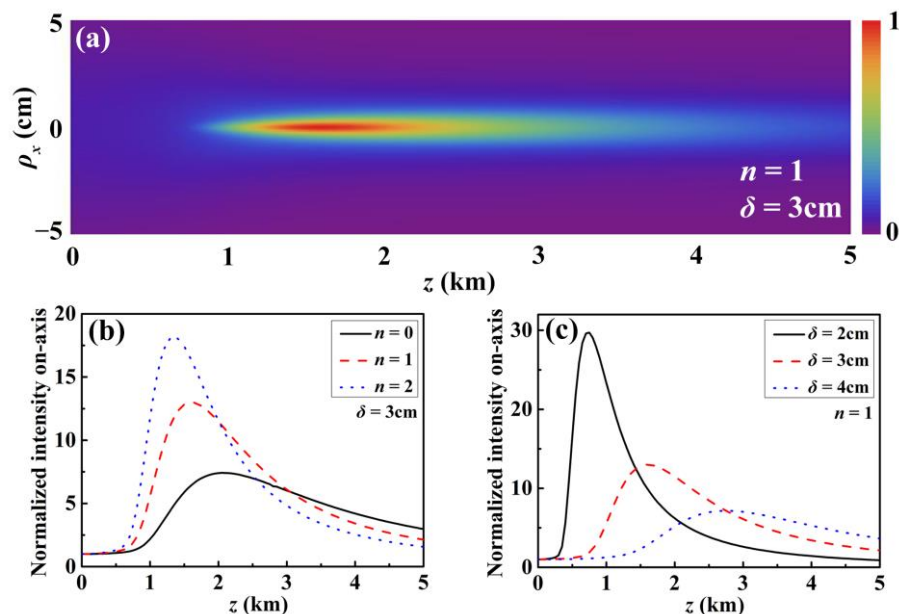


Figure 2. Normalized (a) intensity distribution and (b,c) intensity on-axis of the LNUC beams propagating in free space for (b) different beam orders and (c) coherence lengths.

The evolution of the DOC distribution of the LNUC beams on propagation is depicted in Figure 3. The evolving distribution of coherence exhibits peculiar effects. According to Figures 3a and 1a, the high coherence zone of such a beam is limited to the center of the beams and the two diagonals at the source plane. During propagation in free space, the central part of the high-coherence region decreases, and the two diagonal high-coherence regions increase. With a further increase in propagation, the highly coherence region of DOC gradually expands. Figure 3b,c show the cross-line ( $x_2 = 0$ ) of the DOC at a fitting propagation distance of  $z = 1000$  m for different beam orders and coherence lengths. It is clear from Figure 3b,c that when the LNUC beams with different beam orders and coherence lengths propagate to 1000 m, the reduction in the high-coherence region is different. The increase in beam order and the decrease in coherence will promote the rapid shrinkage of the central high-coherence region, indicating that the propagation characteristics of such beams will be more obvious.

### 3.3. Propagation in Turbulence

Figures 4 and 5 compare the intensity and DOC of the LNUC beams in a turbulent atmosphere. Figure 4 depicts the density plot of the intensity of the beams with different beam orders and coherence lengths, exhibiting self-focusing propagation features in turbulence and the self-focusing characteristics with large beam order and low coherence. The results shown in Figure 4b,c confirm the conclusions initially drawn in Figure 4a. The high-coherence region of the LNUC beams gradually decreases along the diagonal ( $x_1 = x_2$ ) as the propagation distance increases, as shown in Figure 5; with further increase in propagation, the distribution of the DOC along the diagonal in space becomes quasi-homogeneous. Furthermore, Figure 5b,c show the cross-line ( $\rho_{2x} = 0$ ) of the DOC at a fitting propagation distance of  $z = 1000$  m for different beam orders and coherence lengths. The results confirm that the sidelobe distribution of the DOC can be better maintained in low

coherence, suggesting that increasing beam order and decreasing coherence can increase turbulence resistance.

Finally, we focussed on the global parameters of the LNUC beams in turbulence. Figures 6 and 7 depict the plot of the normalized propagation factor and beam wander of the LUNC beams, respectively. Figure 6 confirms that the variation in propagation factor during turbulence increases more slowly with large beam order and low coherence, indicating less impact by turbulence. Figure 7 presents the beam wander of the LNUC beams on propagation during turbulence. Beam wander is reduced in the LNUC beams with high beam order and low coherence.

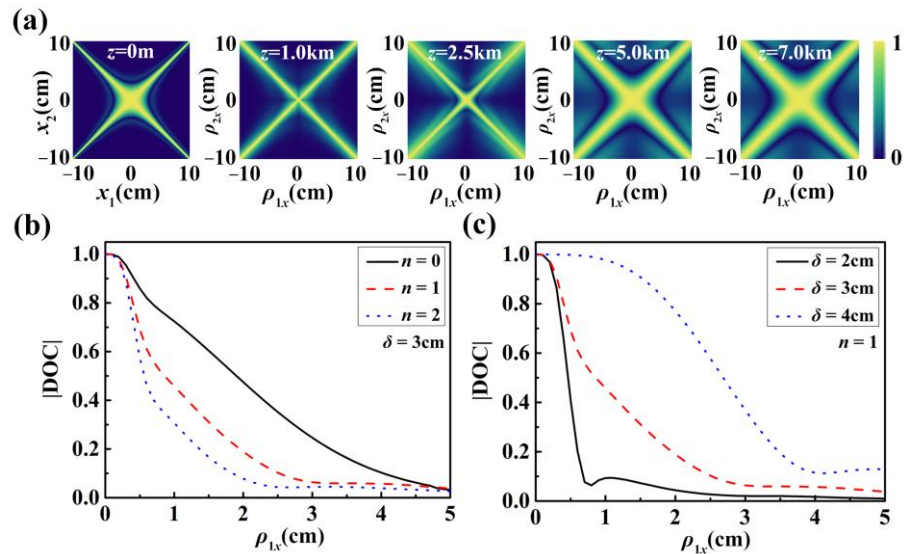


Figure 3. (a) Distribution of the DOC upon propagation in free space and the corresponding cross-line ( $\rho_{2x} = 0$ ) with  $z = 1000\text{ m}$  for (b) different beam orders and (c) coherence lengths.

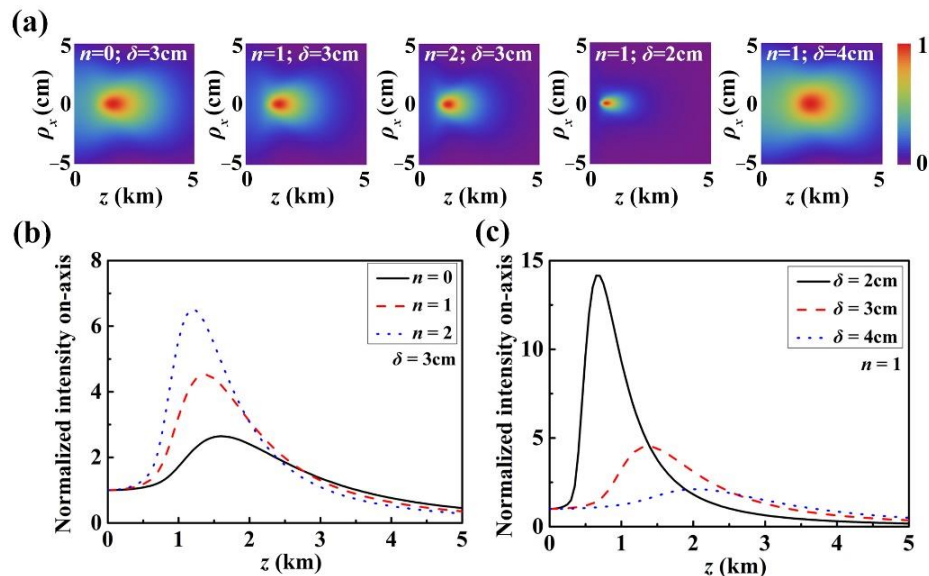
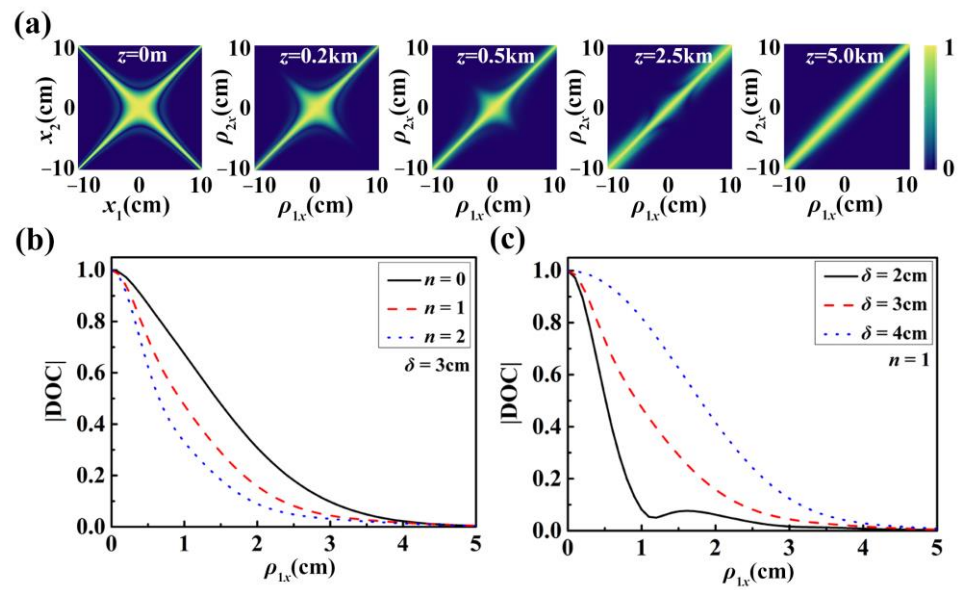
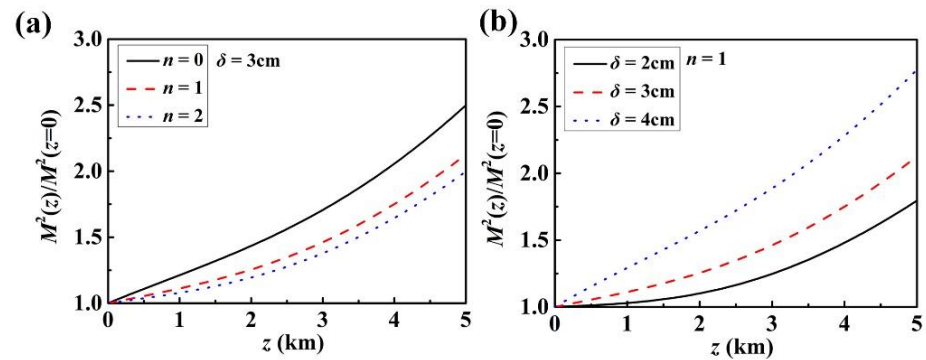


Figure 4. Normalized (a) intensity distribution and (b,c) intensity on-axis of the LNUC beams propagating in turbulence for (b) different beam orders and (c) coherence lengths.



**Figure 5.** (a) Distribution of the DOC upon propagation in turbulence and the corresponding cross-line ( $\rho_{2x} = 0$ ) with  $z = 1000$  m for (b) different beam orders and (c) coherence lengths.



**Figure 6.** Normalized propagation factor in turbulence for (a) different beam orders and (b) coherence lengths.

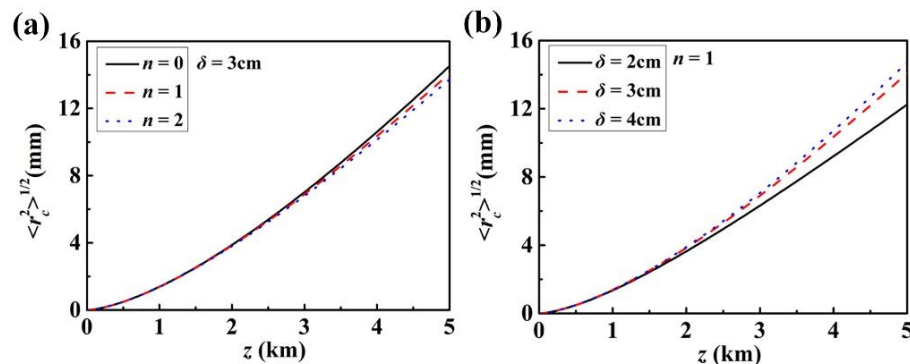


**Figure 7.** Beam wander in turbulence for (a) different beam orders and (b) coherence lengths.

#### 4. Discussion and Conclusions

In this research, the LNUC beams were considered to be a superposition of coherent Gaussian modes with quadratic phase factors. In order to lessen disturbance-based fluctuations and average out turbulent fluctuations, each mode simultaneously travels through a different non-disturbing channel. We could design partially coherent beams with other

novel propagation features based on the present analysis by setting and modifying different coherence modes and weight distributions. This will allow us to determine the best coherence mode and weight distribution to efficiently reduce the detrimental effect caused by turbulence. Future applications of our findings in FSO communication are feasible.

We explored the propagation behavior of LNUC beams in free space and a turbulent atmosphere, exhibiting self-focusing propagation features for both cases. The existence of turbulence negatively impacts the beams, as evidenced by the degenerate evolution of the intensity and DOC. Furthermore, when comparing the evolution of the intensity, correlation structure, propagation factor, and beam wander with different initial beam orders and coherent lengths in turbulence, we found that large beam order and low coherence are less affected by turbulence, implying that increasing the initial beam order and decreasing the initial coherence of the beams can improve their turbulence resistance.

**Author Contributions:** Writing, original draft preparation, Y.Z.; writing, review and editing, J.Y. and B.G.; conceptualization, X.Z.; methodology, X.Z.; software, Z.Y. and Y.W.; data curation, L.L.; supervision, J.Y.; project administration, J.Y. All authors have read and agreed to the published version of the manuscript.

**Funding:** This research was funded by the National Key Research and Development Program of China (2022YFA1404800, 2019YFA0705000); National Natural Science Foundation of China (12192254, 11974218, 12004218, 92250304); China Postdoctoral Science Foundation (2020M680093, 2022M721992); Shandong Provincial Natural Science Foundation of China (ZR2020QA067, ZR2023QA081); The Open Fund of the Guangdong Provincial Key Laboratory of Optical Fiber Sensing and Communications (2020GDSGXCG08).

**Institutional Review Board Statement:** Not applicable.

**Informed Consent Statement:** Not applicable.

**Data Availability Statement:** Data are contained within the article.

**Conflicts of Interest:** The authors declare no conflict of interest.

## References

1. Forbes, A.; Oliveira, M.D.; Dennis, M.R. Structured light. *Nat. Photonics* **2021**, *15*, 253–262. [[CrossRef](#)]
2. Mandel, L.; Wolf, E. *Optical Coherence and Quantum Optics*; Cambridge University: Cambridge, MA, USA, 1995.
3. Cai, Y.; Chen, Y.; Yu, J.; Liu, X.; Liu, L. Generation of partially coherent beams. *Prog. Opt.* **2017**, *62*, 157–223.
4. Korotkova, O.; Gbur, G. Applications of optical coherence theory. *Prog. Opt.* **2020**, *65*, 43–104.
5. Chen, Y.; Wang, F.; Cai, Y. Partially coherent light beam shaping via complex spatial coherence structure engineering. *Adv. Phys. X* **2022**, *7*, 2009742. [[CrossRef](#)]
6. Gori, F.; Santarsiero, M. Variant-coherence Gaussian sources. *Photonics* **2021**, *8*, 403. [[CrossRef](#)]
7. Martínez-Herrero, R.; Santarsiero, M.; Piquero, G.; González de Sande, J.C. A new type of shape-invariant beams with structured coherence: Laguerre-Christoffel-Darboux beams. *Photonics* **2021**, *8*, 134. [[CrossRef](#)]
8. Ding, C.; Korotkova, O.; Horoshko, D.; Zhao, Z.; Pan, L. Evolution of Spatiotemporal Intensity of Partially Coherent Pulsed Beams with Spatial Cosine-Gaussian and Temporal Laguerre–Gaussian Correlations in Still, Pure Water. *Photonics* **2021**, *8*, 102. [[CrossRef](#)]
9. Sun, B.; Lü, H.; Wu, D.; Wang, F.; Cai, Y. Propagation of a modified complex Lorentz–Gaussian-correlated beam in a marine atmosphere. *Photonics* **2021**, *8*, 82. [[CrossRef](#)]
10. Andrews, L.C.; Phillips, R.L. *Laser Beam Propagation through Random Media*, 2nd ed.; SPIE: Bellingham, DC, USA, 2005; pp. 35–56.
11. Peng, D.; Huang, Z.; Liu, Y.; Chen, Y.; Wang, F.; Ponomarenko, S.A.; Cai, Y. Optical coherence encryption with structured random light. *Photonix* **2021**, *2*, 6–15. [[CrossRef](#)]
12. Liu, Y.; Chen, Y.; Wang, F.; Cai, Y.; Liang, C.; Korotkova, O. Robust far-field imaging by spatial coherence engineering. *Opto-Electron. Adv.* **2021**, *4*, 210027. [[CrossRef](#)]
13. Tatarski, V.I. *Wave Propagation in a Turbulent Medium*; Courier Dover Publications: Mineola, NY, USA, 2016.
14. Gbur, G. Partially coherent beam propagation in atmospheric turbulence. *J. Opt. Soc. Am. A* **2014**, *31*, 2038–2045. [[CrossRef](#)]
15. Wang, F.; Liu, X.; Cai, Y. Propagation of partially coherent beam in turbulent atmosphere: A review (Invited review). *Prog. Electromagn. Res.* **2015**, *150*, 123–143. [[CrossRef](#)]
16. Ponomarenko, S.A. A class of partially coherent beams carrying optical vortices. *J. Opt. Soc. Am. A* **2001**, *18*, 150–156. [[CrossRef](#)]
17. Lajunen, H.; Saastamoinen, T. Propagation characteristics of partially coherent beams with spatially varying correlations. *Opt. Lett.* **2011**, *36*, 4104–4106. [[CrossRef](#)]

18. Yu, J.; Wang, F.; Liu, L.; Cai, Y.; Gbur, G. Propagation properties of Hermite non-uniformly correlated beams in turbulence. *Opt. Express* **2018**, *26*, 16333–16343. [[CrossRef](#)]
19. Yu, J.; Cai, Y.; Gbur, G. Rectangular Hermite nonuniformly correlated beams and its propagation properties. *Opt. Express* **2018**, *26*, 27894–27906. [[CrossRef](#)]
20. Yu, J.; Zhu, X.; Lin, S.; Wang, F.; Gbur, G.; Cai, Y. Vector partially coherent beams with prescribed non-uniform correlation structure. *Opt. Lett.* **2020**, *45*, 3824–3827. [[CrossRef](#)]
21. Gori, F.; Santarsiero, M. Devising genuine spatial correlation functions. *Opt. Lett.* **2007**, *32*, 3531–3533. [[CrossRef](#)]
22. Gu, Y.; Gbur, G. Scintillation of nonuniformly correlated beams in atmospheric turbulence. *Opt. Lett.* **2013**, *38*, 1395–1397. [[CrossRef](#)]
23. Lin, S.; Wang, C.; Zhu, X.; Lin, R.; Wang, F.; Gbur, G.; Cai, Y.; Yu, J. Propagation of radially polarized Hermite non-uniformly correlated beams in a turbulent atmosphere. *Opt. Express* **2020**, *28*, 27238–27249. [[CrossRef](#)]
24. Yu, J.; Xu, Y.; Lin, S.; Zhu, X. Longitudinal optical trapping and manipulating Rayleigh particles by spatial nonuniform coherence engineering. *Phys. Rev. A* **2022**, *106*, 033511. [[CrossRef](#)]
25. Dan, Y.; Zhang, B. Second moments of partially coherent beams in atmospheric turbulence. *Opt. Lett.* **2009**, *34*, 563–565. [[CrossRef](#)] [[PubMed](#)]
26. Martínez-Herrero, R.; Mejías, P.M.; Piquero, G. Quality improvement of partially coherent symmetric-intensity beams caused by quartic phase distortions. *Opt. Lett.* **1992**, *17*, 1650–1651. [[CrossRef](#)] [[PubMed](#)]
27. Gori, F.; Santarsiero, M.; Sona, A. The change of width for a partially coherent beam on paraxial propagation. *Opt. Commun.* **1991**, *82*, 197. [[CrossRef](#)]
28. Xiao, X.; Voelz, D. Beam wander analysis for focused partially coherent beams propagating in turbulence. *Opt. Eng.* **2012**, *51*, 026001. [[CrossRef](#)]
29. Toselli, I.; Andrews, L.C.; Phillips, R.L.; Ferrero, V. Free-space optical system performance for laser beam propagation through non-Kolmogorov turbulence. *Opt. Eng.* **2008**, *47*, 026003.

**Disclaimer/Publisher’s Note:** The statements, opinions and data contained in all publications are solely those of the individual author(s) and contributor(s) and not of MDPI and/or the editor(s). MDPI and/or the editor(s) disclaim responsibility for any injury to people or property resulting from any ideas, methods, instructions or products referred to in the content.